Autonomous Craters Detection from Planetary Image

Ding Meng[1]   Cao Yun-feng[1,2]   Wu Qing-xian[1]

[1](School of Automatic Engineering，NanJing University of Aeronautics and Astronautics)

[2](Academy of Frontier Science，NanJing University of Aeronautics and Astronautics)

Abstract

As development of deep space exploration, the Guidance, Navigation and Control (GNC) technology of spacecraft or probe is becoming more important than ever. Vision-based navigation (optical navigation) is a good method to achieve autonomous landing of spacecraft. Therefore, the landmark has to be detected for Vision-based navigation. Craters are commonly found on the surface of planets, satellites, asteroids and other solar system bodies. Currently, the most of optical landmark navigation algorithm are built on the craters detection and tracking. The focus of this paper is to present an algorithm for autonomous crater detection. The whole course of crater detection can be divided into two steps, Multi-resolution feature points extraction and crater detection. The first step can be further divided into Multi-resolution window-based feature points' extraction and crater candidate area choice. The second step can be further divided into region growing, pixels of crater edge extraction, ellipse detection and obtaining craters. Experimental studies demonstrate that the detection rate of this algorithm is higher than 90% for image where the distribution of craters is discrete.

I. INTRODUCTION AND BACKGROUND

Craters are commonly found on the surface of planets, satellites, asteroids and other solar system bodies. The number and size of craters can establish the age of the surface or surface units and yield the relative ages between the surfaces of different bodies. Generally, the crater is a bowl shaped depression created by collision or volcanic activities. Younger craters may have sharper and regular rims while aged craters might have very vague rims. Therefore, the craters are a fundamental tool to determinate the geological age and history of a surface.

Because of the communication delay between earth and planets, satellites, asteroids and other solar system bodies, the Guidance, Navigation and Control(GNC) technology of spacecraft or probe is becoming more important than ever. Current navigation technology is not able to provide precise motion estimation for probe landing control system Computer vision(optical navigation) offers a new approach to solve this problem[1]-[3]. Jet Propulsion Laboratory(JPL)'s Descent Image Motion Estimation System(DIMES) is the first optical navigation in the world for probe landing. On 4 January and 25 June 2004. DIMES measured precise horizontal velocity for MER-A and MER-B safely landing on the Mars. The successful performance of DIMES has shown that it is possible to autonomously process and react to imagery during landing on the Mars[4]. Feature detection and tracking is the first and important step for spacecraft or probe optical navigation. A.Johnson from JPL chooses feature points which is the window has strong texture variations in all directions to track[5]. Japanese researcher Toshihiko Misu offers an algorithm based on fixation area, which fixates on the areas with local varying intensity, and employs shading pattern as a fixation area, and then tracked the center of the fixation area[6]. Craters are also ideal feature for spacecraft or probe optical navigation. Optical landmark navigation using craters on the surface of a central body was first used operationally by the Near Earth Asteroid Rendezvous (NEAR), rendezvoused with asteroid Eros 433 in February 2000. NEAR mission's success has proven crater tracking is a powerful data type for spacecraft orbit determination in low altitude orbits[7].

There are many surface hazards in the form of craters, rocks, faults, ridges, and channels existing over the entire surface of solar system bodies. Landing a spacecraft or probe safely on a body surface autonomously requires the ability to detect and avoid hazards on the surface. JPL developed an algorithm for safe landing on Mars based LIDAR to avoid hazard and select a safe landing site[8]. An optical camera is one of several different types of sensors that can be used to achieve this capability. While it does not explicitly provide range data like RADAR or LIDAR sensors, it has the advantages of a larger field of view, less power consumption, light weight, better resolution, and fewer mechanical components subject to failure[9]. Therefore, it is important to develop an image process and pattern recognition algorithm for hazards detection.

A very robust and powerful crater detection algorithm has been developed by the JPL Machine Vision Group. The algorithm is broken down into six steps: Edge Detection, Crater anchor point detection, Rim edge grouping, Ellipse fitting, Ellipse refinement and Crater confidence evaluation. Experimental studies show that this algorithm can achieve sub-pixel accuracy in position, its detection rate is better than 90% and its false alarm rate is less than 5%[10].

Among the some other different approaches worthy of mention, some have used template matching[11][12][13], Image pixel arrays are rotated, translated or otherwise transformed to match piece of an image, Such as M.C.Burl's Continuously Scalable Template Matching algorithm. Tests show that this algorithm achieves an 80% probability of detection for craters larger than four pixels in diameter at a 12% false alarm rate.

Some have use Hough Transform for crater detection because of their relative simple and regular geometries. The principle idea of the method is to compute a number a parameter space that defines the shape

detect)and an image space. In 1999, Honda developed a crater detection algorithm based on Generalized Hough Transform (GHT)[14]. An ellipse detection method based on GHT was also used for carter detection on asteroids for spacecraft position estimation[5] and choosing a landing site[8]. However, when applying this method to conic curves with many degrees of freedom, such as an ellipse(5 degrees of freedom), large computation makes this approach too expensive.

Some have employed texture analysis for crater detection [6][15]. They calculate variance in each tile and use shadows(high local variance) to detect crater or rocks. Still other algorithms are used for identification of craters. However, the results presented were far from being good enough to convince the deep space exploration research group to adopt many of these approaches.

This paper demonstrates an algorithm for crater detection based on feature points and ellipse detection. In section 2, Multi-resolution window-based KTL feature point extracting algorithm is employed for candidate area of crater decision. Some image processing methods are used to detect the craters and calculate parameters of ellipse in section3. The entire course of algorithm is described in table 1.

II. MUITI-RESOLUTION FEATURE POINTS EXTRACTION

From Figure1.a, We can find that a typical crater in an image has an elliptical rim and a bright to dark shading Pattern and inside of it the image intensity profile along lighting direction should be a monotonously decreasing function. Therefore, if the photograph is shot in certain altitude, intensity variations are strong in the region of craters(Fig1.b,c).
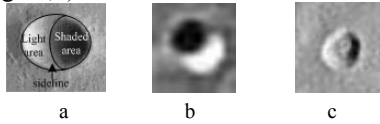

a   b   c
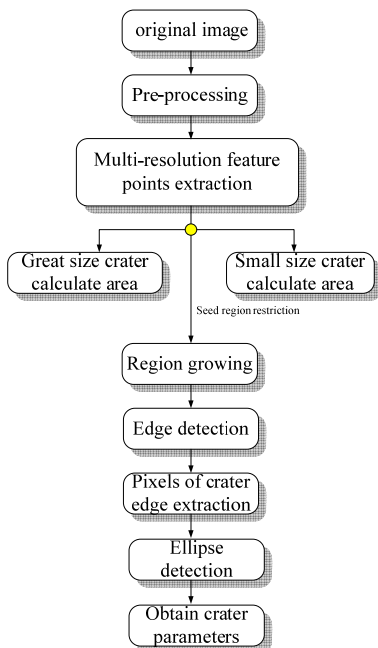
Fig1. Typical Craters

Table1. Structure of algorithm

2.1 Feature Points Extraction

We know that a good feature is a feature window which has strong variation in directs. Thus the craters are the good features which can be extracted by some feature points(FP) detection algorithms. In this paper, FPs do not mean only a pixel of high intensity, but although a serious of feature windows minimum size is 7×7. Many algorithms about FPs detection have been described in literatures. Generally, they are divided into two groups. The first group involves extracting edges and then finding the points with maxima curvature or searching for points where edge segments intersect. The second and largest group consists of algorithms that search for corners directly from the grey-level image[16]. In the second group, there are four most classical methods: Kanade-Lucas-Tomasi (KLT)[17], the Harris algorithm, the Kitchen-Rosenfeld and the Smith feature points detection. Kitchen-Rosenfeld algorithm is one of the earliest corner detectors reported in the literature. The Harris detector is based on an underlying assumption that corners are associated with maxima of the local autocorrelation function. The KLT corner detector operates by comparing a patch of image information in two consecutive frames of an image sequence which is developed for feature tracking. Paper[16] shows that KLT is a better method to detect feature points in nature environment. Consequently, in this paper, KLT is used for crater primary detection. The algorithm is expressed simply as follows:

Step1.Computing the image gradient across the image at each pixel location

$$I_x(x,y,t) = \frac{I(x+1,y) - I(x-1,y)}{2}$$
$$I_y(x,y,t) = \frac{I(x,y+1) - I(x,y-1)}{2}$$

$I(x,y,t)$ denoted the continuous function defining the brightness values of a sequence of images captured by a camera. The partial derivatives of $I(x,y,t)$ with respect to x, y, are denoted respectively by $I_x(x,y,t)$ and $I_y(x,y,t)$.

Step2.Defining matrix G

$$G = \begin{bmatrix} \sum_{W_1}(I_x(x,y,t))^2 & \sum_{W_1}I_x(x,y,t)I_y(x,y,t) \\ \sum_{W_1}I_x(x,y,t)I_y(x,y,t) & \sum_{W_1}(I_y(x,y,t))^2 \end{bmatrix} = \begin{bmatrix} a & b \\ b & c \end{bmatrix}$$

W1 denoted feature patch of pixels including pixel point(x,y).

Step3. Find $\lambda_1(i,j)$, every image pixel with the minimum eigenvalue.

Step4. Discard any pixel with $\lambda_1(i,j) < \lambda_t$;

The exhaustive search strategy is used to compute every pixel according to this algorithm for crater detection.

2.2 Multi-resolution FPs Extraction and Candidate Area Decision

The definition of Multi-resolution is that different size of W1 is selected to define matrix G and then calculate minimum eigenvalue. Intensity variations are strong in the whole region of crater, therefore great size craters need great size feature patch to detect and the small ones need small feature patch. In fact, the purpose of Multi-resolution is to ensure one FP corresponding to each crate

IEEE
computer
society

and its size is equal to W1. The process of Multi-resolution extraction is expressed simply as follows:

Step1. The primary size of W1(d_0) is ensured. Generally d_0 is a biggish odd number.

Step2. KLT Feature points extraction.

Step3. $d_i = d_{i-1} - 2$, return step2, if new feature points are extracted in feature patch which has been detected, delete new points and keep the size of original patch as the size of candidate area. If the location of FP is invariable by different size of W1 extracting, choose minimum size of W1 as size of candidate area.

Step4. End, until $d_i = 7$; This step means the algorithm can detect craters of minimum size 7×7. If we choose too small size of W1, the noise of image may induce erroneous FPs are detected.

In Fig2, there are some different size craters. The feature points based on different size of W1 are computed and the location of Feature points is shown in Fig3, the size of blue rectangles present the size feature patches (candidate area) which have been detected. Table2 illuminates the sizes of feature patches.
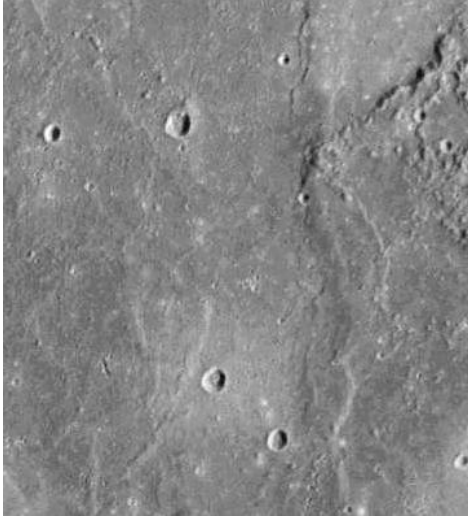

Fig2. Surface of original moon images, craters of different size are shown clearly.
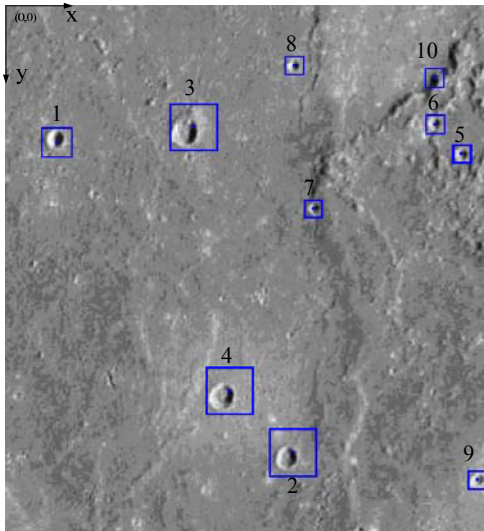

Fig3. Results of Multi-resolution FPs extraction(λ_t =1000, blue points present Fps)

Num	Location of FPs	Size of feature patch
1	(40,107)	25×25
2	(218,336)	41×41
3	(143,93)	41×41
4	(218,336)	41×41
5	(344,113)	15×15
6	(324,91)	15×15
7	(233,154)	15×15
8	(219,47)	15×15
9	(357,356)	13×13
10	(324,47)	15×15

Table2. Sizes of feature patches and location of FPs

Before crater detection, the 5*5 median filter is used for noise reduction and the original image is blurred due to the small size of craters can't be extracted synchronously.

III. CRATER DETECTION

The crater can be divided into two parts, shaded area and light area. In this section, this classic characteristic of crater is used to detect crater from candidate area.

3.1 Region Growing

Commonly, the image thresholding as a central position in application of image segmentation is used to extract the object of interest from background. The choice of threshold value has been discussed in many algorithms. However, this is also the most difficult point of image thresholding. Because of including two parts, the crater detection based on threshold segmentation requires multiple thresholds. In general, segmentation problem requiring multiple thresholds are best solved using region growing method[18]. As its name implies, region growing is a procedure that group pixels or sub-region into larger regions based on predefined criteria. The basic approach is starting with a set of "seed" points and from these grow regions by appending to each seed those neighboring pixels that have properties similar to the seed(such as specific ranges of gray level). Two problems, the choice of seed and the criteria of grouping pixels into larger regions have to be solved for region growing.

The process of region growing is expressed simply as follows:

Step1. Pre-process every candidate area(the feature patch which has been detected in section 2).

From Fig4, we can find that the pixels of max and min intensity value in every candidate area are inside the crater. Histogram Equalization as pre-processing is used to make sure the gray level of every candidate area is uniformly distributed.

Step2. The pixels of max and min intensity value of candidate area are selected as seeds. Sometimes, those pixels may appear along the edge of candidate area, the location of FPs is used to guarantee those pixels are exclusive of the seeds for region growing.

Step3. The criteria of region growing based on the pixel of gray level.

$$| g_s - g_c |< threshold$$

Where, g_s is the gray value of seed and g_c is the gray value of candidate pixel.

We choose one feature patch from Fig1.b and the result of process is in Fig4a.b. Two closed continuous curves of Fig4.b include edges of craters and the sideline which is a boundary between the shaded part and light part. The next work is to extract the edges and delete the sideline of crater for the ellipse detection.
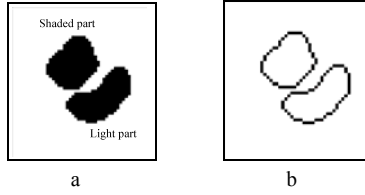

Fig4. Feature pitch including crater and the result of region growing. (Threshold=15)

3.2 Pixels of Crater Edge Extraction

To detect the ellipse of crater, the edge of crater must be extracted firstly. The process is expressed simply as follows:

Step1. Calculate pitch of crater.

The definition of pitch is shown in Fig5. the pitch of crater is an angle between line of two points(the center point of shaded part (x_{0S}, y_{0S}) and light part (x_{0L}, y_{0L})) and U axis of image pixel coordinate frame.

$$x_{0L} = \frac{\sum_{i=1}^{n} x_{iL}}{n}, y_{0L} = \frac{\sum_{i=1}^{n} y_{iL}}{n} \quad x_{0S} = \frac{\sum_{i=1}^{n} x_{iS}}{n}, y_{0S} = \frac{\sum_{i=1}^{n} y_{iS}}{n}$$

Where, (x_{iL}, y_{iL}), (x_{iS}, y_{iS}) is the coordinate value of light part and shaded part.

$$\theta = \tan^{-1}(\frac{y_{L0} - y_{S0}}{x_{L0} - x_{S0}})$$

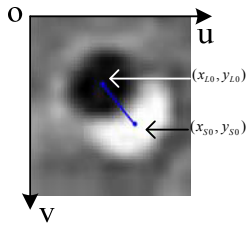Fig5. Pitch of crater($\theta = 49.938°$)

Step2. Obtain pixels of crater edge.

Make Fig4.b clockwise rotate $90 - \theta$. Scan every row of new image matrix and keep the first and last pixel of value=0, the others=1(result is shown in Fig6). This step saves the pixel of edge and deletes the pixel of sideline.
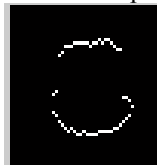

Fig.6 Edge of crater which has been extracted

3.3 Ellipses Detection

For an arbitrary ellipse, there are five unknown parameters, (x_0, y_0) for the center, ϕ for the orientation, (a, b) for the major and minor axes. Usually we need a five dimensional parameter space to detect an ellipse. That is very memory and time consuming. Usually the methods of detecting ellipse can be divided into four kinds: improved

Hough Transform[19], GA-based method, statistical method[20] and improved K-RANSAC. The key idea of those methods is to use some geometric constraints to reduce the complexity of the parameter space. In this paper, we use an algorithm based on statistics theory to detect circle and ellipse quickly and synchronously. According to the definition of error ellipse in statistics, the max and min positional error of a given point in two-dimensional space are the semi-major and semi-minor axis of error ellipse. Built on this principle, the algorithm is expressed simply as follows:

Step1: calculate (x_0, y_0) for the center

$$\begin{cases} x_0 = \dfrac{\sum_{i=1}^{n} x_i}{n} \\ y_0 = \dfrac{\sum_{i=1}^{n} y_i}{n} \end{cases}$$

(x_i, y_i) is the edge point.

Step2: Defining matrix D

$$D = \begin{bmatrix} \dfrac{\sum_{i=1}^{n}(x_i - x_0)^2}{n} & \dfrac{\sum_{i=1}^{n}(x_i - x_0)(y_i - y_0)}{n} \\ \dfrac{\sum_{i=1}^{n}(x_i - x_0)(y_i - y_0)}{n} & \dfrac{\sum_{i=1}^{n}(y_i - y_0)^2}{n} \end{bmatrix}$$

Step3: calculate eigenvalues of matrix D

$$\lambda_{1,2} = 0.5(D_{11} + D_{22} \pm K),$$

Where K is

$$K = \sqrt{(D_{11} - D_{22})^2 + 4D_{12}^2}$$

Step4: (a, b) for the major and minor axes are:

$$a = \sqrt{\lambda_1}, b = \sqrt{\lambda_2}$$

Obviously, $\phi = 90°$. When the ellipses have been detected, ellipse including whole crater can be gained by contra-rotating this ellipse $90 - \theta$. The final result is shown in Fig7. We should notice that the ellipse of $a/b > 4$ does not include craters. That is why the 10th candidate area of Fig3 without crater.
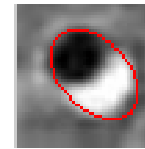

Fig.7 Extracted crater from Fig1.b

Altogether, the whole process of crater detection can be divided into five steps: region growing, edge detection, extracting edge pixels of crater, ellipse detection and crater obtaining.

IV. EXPERIMENT AND RESULTS

We use this algorithm to process Fig2 and the crater candidate areas have been shown in Fig3 (the number of candidate areas is 10). In Fig8, the final results of crater detection are shown. Compared with Fig3, only one candidate area does not include crater. The parameters of ellipses are demonstrated in table3.
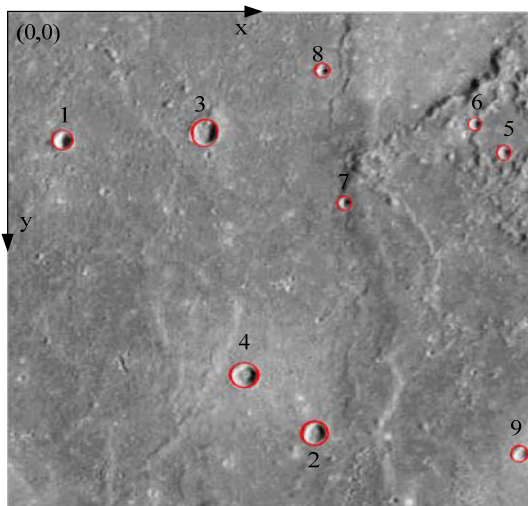
IEEE
@computer society

Fig8. Final results of crater detection

Num	(x_0, y_0)	a	b	$\phi°$
1	(38,103)	44	39	9.5451
2	(212,339)	58	52	-17.45
3	(137,98)	82	53	-13.447
4	(164,293)	68	61	-14.467
5	(343,113)	21	14	-3.8914
6	(324,91)	22	14	-1.9926
7	(233,154)	20	14	-13.315
8	(218,47)	22	15	8.9644
9	(354,356)	28	21	-2.1106

Table3. Parameters of ellipses

V. CONCLUSION

For Fig4, the detection rate of this algorithm presented in this paper is almost 100%. Many experiments show that the detection rate is higher than 90% in the simulative artificial perfect environment. For the real moon's surface images where the distribution of craters is discrete, the detection rate is higher than 90%.

We can also find that this algorithm can be improved in some aspects. The further work should improve the choice method of seed and use some intelligent methods to decide the size of crater candidate area.

Acknowledgements

REFERENCES

[1] J Kawaguchi, J., Hashimoto, T., Kubota, T., Sawai, S., and Fujii, G. (1997) Autonomous optical guidance and navigation strategy around a small body. AIAA Journal of Guidance, Control, and Dynamics, 20, 5(Sept.—Oct. 1997), 1010—1017.

[2] Yang Cheng et al, "Autonomous Landmark Based Spacecraft Navigation System", AAS/AIAA Space Flight Mechanics Meeting Feb 9-13, 2003. Vol.114 Pt.III; 2003; Ponce, Puerto Rico

[3] Andrew E.Johnson et al "Machine Vision for Autonomous Small Body Navigation ", 2000 IEEE Aerospace Conference, vol.7, Big Sky, Montana, USA, March 18-25, 2000.

[4] Yang Cheng et al, "The Mars Exploration Rovers Descent Image Motion Estimation System" IEEE Intelligent Systems, May/June 2004, 13-21.

[5] Andrew E.Johnson.Larry and H.Matthies, "Precise Image-Based Motion Estimation for Autonomous Small Body Exploration". 5th International Symposium on Artificial Intelligence and Automation in Space,Noordwijk,June 1999:627-634.

[6] Toshihiko Misu et al, "Optical Guidance for Autonomous Landing of Spacecraft", IEEE Transactions on Aerospace and Electronic Vol. 35, No. 2 April 1999

[7] J.K. Miller et al."Navigation analysis For Eros rendezvous and orbital phases." Journal Astronautical Sciences, vol.43, No.4, pp.453-476.1995

[8] Andrew E.Johnson, A. Klump, J. Collier, and AronWolf, "LIDAR-Base Hazard Avoidance for Safe Landing on Mars," AAS/AIAA Space Flight Mechanics Meeting, Santa Barbara, CA,February 2001.

[9] Max Bajracharya, "Single image Based Hazard Detection for A Planetary Lander", 5th Biannual World Automation Congress (WAC 2002); 2002; Orlando, Florida, USA;

[10] Yang Cheng et al, "Optical Landmark Detection for Spacecraft Navigation". 13th AAS/AIAA Space Flight Mech.Meet, 2003

[11] M.C.Burl et al, "Automated Detection of Craters and Other Geological Features", Proc.I-SAIRAS-01,monreal,Canada,june 2001.

[12] Michael et al, "Coordinate Registration by Automated Crater Recongnition", Planetary and Space Science 51, 563-568(2003)

[13] Lourenco P.C. Banderia et al," Development of a Methodology for Automated Crater Detection on Planetary Images", Pattern recognition and image analysis; 2007; Gerona, Spain.

[14] Honda et al, "Data Mining System for Planetary Images-Crater Detection and Categorization" 1999.

[15] Barata et al, "Automatic Recognition of Impact Crater Detection on the surface of Mars". In: Campilho, A.Kamel, ICIAR2004.pp489-496. Springer, Heidelberg, 2004.

[16] P.Tissainayagam et al, Assessing the performance of corner detectors for point feature tracking applications: Image and Vision computing 22(2004),663-679.

[17] A.Benedetti, P.Perona. Real-time 2-D Feature Detection on a Reconfigurable Computer. IEEE Conf. Computer Vision and Pattern Recognition,1998:586-593.

[18] Rafael C.Gonzalez et al, Digital Image Processing, Publishing House of Electronics

[19] E. R. Davies, Finding ellipses using the generalized Hough transform, Pattern Recog. Lett. 9, 1989, 87--96.

[20] Qiang Ji and Robert M. Haralick, A Statistically Efficient Method for Ellipse Detection, in 1999 IEEE International Conference on Image Processing, Kobe, Japan, October, 1999.

Ding Meng received B.E. and M.E degrees in School of Automatic Engineering, NanJing University of Aeronautics and Astronautics in 2003 and 2006. He is currently working toward Ph.D. in the same university. His interests are Computer Vision and Pattern Recognition.
Phone: 86-025-84890902;
E-mail: nuaa_dm@hotmail.com.

Cao Yun-feng received M.E in School of Automatic Engineering, NanJing University of Aeronautics and Astronautics in 1996. Now, he is the professor in Academy of Frontier Science of NanJing University of Aeronautics and Astronautics. His interests are Flight Control System and Intelligence Control.

Wu Qing-xian received M.E from Southeast University in 1985. Now, he is the professor in School of Automatic Engineering of NanJing University of Aeronautics and Astronautics. His interests are intelligence control and Pattern Recognition.

IEEE
computer society